A comparative study of optical and radiative characteristics of X-ray-induced luminescent defects in Ag-doped glass and LiF thin films and their applications in 2-D imaging

doi: 10.1016/j.nimb.2013.08.011

Elsevier Editorial System(tm) for NIMB Proceedings
Manuscript Draft

Manuscript Number:

Title: A comparative study of optical and radiative characteristics of X-ray-induced luminescent defects in Ag-doped glass and LiF thin films and their applications in 2-D imaging

Article Type: Proc: REI 2013

Section/Category: Proc: REI2013

Keywords: Glass dosimeter, X-ray imaging, RPL, PL, OSL, LiF thin film

Corresponding Author: Prof. Toshio Kurobori,

Corresponding Author's Institution:

First Author: Toshio Kurobori, Prof.

Order of Authors: Toshio Kurobori, Prof.; Yuka Miyamoto, Dr.; Yoichi Maruyama, Mr.; Takayoshi Yamamoto, Prof.; Toshihiko Sasaki, Prof.

Abstract: ABSTRACT
We report novel disk-type X-ray two-dimensional (2-D) imaging detectors utilising Ag-doped phosphate glass and lithium fluoride (LiF) thin films based on the radiophotoluminescence (RPL) and photoluminescence (PL) phenomena, respectively. The accumulated X-ray doses written in the form of atomic-scale Ag-related luminescent centres in Ag-doped glass and F-aggregated centres in LiF thin films were rapidly reconstructed as a dose distribution using a homemade readout system. The 2-D images reconstructed from the RPL and PL detectors are compared with that from the optically stimulated luminescence (OSL) detector. In addition, the optical and dosimetric characteristics of LiF thin films are investigated and evaluated. The possibilities of dose distributions with a high spatial resolution on the order of microns over large areas, a wide dynamic range covering 11 orders of magnitude and a non-destructive readout are successfully demonstrated by combining the Ag-doped glass with LiF thin films.

Toshio KUROBORI

HIGHLIGHTS

- A novel disk-type Ag-doped glass and LiF thin film detectors based on the RPL and PL phenomena, respectively, were proposed.
- The capabilities of the 2-D dose images accumulated with a high spatial resolution and a wide dynamic range were demonstrated.
- The 2-D images reconstructed from the RPL and PL detectors were compared with that from the OSL detector.

A comparative study of optical and radiative characteristics of X-ray-induced luminescent defects in Ag-doped glass and LiF thin films and their applications in 2-D imaging

T. Kurobori [a,*], Y. Miyamoto [b], Y. Maruyama [a, c], T. Yamamoto [b], T. Sasaki [a]

[a] *Graduate School of Natural Science and Technology, Kanazawa University, Kakuma-machi, Kanazawa, Ishikawa 920-1192, Japan*

[b] *Oarai Research Center, Chiyoda Technol Corporation, 3681 Narita-cho, Oarai-machi, Ibaraki 311-1313, Japan*

[c] *Pulstec Industrial Corporation, 7000-35 Nakagawa, Hosoe-cho, Kita-ku, Hamamatsu-shi, Shizuoka, 431-1304, Japan*

ABSTRACT

We report novel disk-type X-ray two-dimensional (2-D) imaging detectors utilising Ag-doped phosphate glass and lithium fluoride (LiF) thin films based on the radiophotoluminescence (RPL) and photoluminescence (PL) phenomena, respectively. The accumulated X-ray doses written in the form of atomic-scale Ag-related luminescent centres in Ag-doped glass and F-aggregated centres in LiF thin films were rapidly reconstructed as a dose distribution using a homemade readout system. The 2-D images reconstructed from the RPL and PL detectors are compared with that from the optically stimulated luminescence (OSL) detector. In addition, the optical and dosimetric characteristics of LiF thin films are investigated and evaluated. The possibilities of dose distributions with a high spatial resolution on the order of microns over large areas, a wide dynamic range covering 11 orders of magnitude and a non-destructive readout are successfully demonstrated by combining the Ag-doped glass with LiF thin films.

Keywords:
Glass dosimeter, X-ray imaging, RPL, PL, OSL, LiF thin film

[*]Corresponding author. fax: +81-76-234-4132.
[*] *E-mail address*: kurobori@staff.kanazawa-u.ac.jp.

1. Introduction

Radiophotoluminescent (RPL) glass dosimeters [1] using silver-activated phosphate glass have been widely used for personal, environmental and clinical dosimetry, along with optically stimulated luminescence (OSL) dosimeters [2] and thermoluminescent (TL) dosimeters [3, 4]. In particular, the RPL dosimeter has been recognised as possessing desirable characteristics such as high spatial resolution, non-destructive readout capabilities, a long-term stability against fading, a wide dynamic range and uniformity/batch homogeneity [5]. Although these three passive types of luminescent dosimeters, based on the RPL, OSL and TL (referred to by their well-known abbreviations for convenience) phenomena, have advantages and disadvantages [3, 6], there have been few reports of two-dimensional (2-D) dose distributions achieved over large areas with the aforementioned features.

Several reports have demonstrated stored micro-images written by extreme ultraviolet (EUV) rays, soft and hard X-rays, neutrons, high-energy heavy charged particles and alpha-particles using radiation-induced centres or stable aggregate colour centres (CCs) in transparent materials.

Firstly, although lithium fluoride (LiF) crystals doped with magnesium and titanium (LiF:Mg, Ti) are well known to function as TL detectors, it is difficult to adopt such TL phenomena to 2-D imaging due to a lack of repeatable readouts. However, stable F_2 and F_3^+

CCs, whose centres consist of two electrons bound to three or two adjacent anion vacancies, respectively, embedded in LiF crystals and films based on the photoluminescence (PL) phenomenon can be used for high-performance detectors in micro-radiography, X-ray microscopy and phase contrast imaging [7-9]. Secondly, stable F_2^{2+} (2Mg) CCs in aluminium oxide doped with carbon and magnesium (Al_2O_3:C, Mg) crystals based on the OSL phenomenon have been used as a fluorescent nuclear track detector [10]. Thirdly, radiation-induced silver species such as stable Ag^{2+} or Ag^0 CCs in Ag-doped glass based on the RPL phenomenon can be used in microscopic dose measurements [11]. However, all of the aforementioned image types are optically read by a confocal laser scanning microscope (CLSM). Consequently, these methods are less suitable for measuring large-area images, particularly, in medical dosimetry applications or in outdoor environments, e.g., in structural health monitoring for buildings, tunnels and bridges.

In this paper, novel disk-type X-ray 2-D imaging detectors utilising Ag-doped phosphate glass and LiF thin films deposited on glass based on the RPL and PL phenomena, respectively, are proposed and demonstrated for applications in diagnostic dosimetry and radiation therapy. The capabilities of the reconstructed dose distributions with a wide dynamic range covering 11 orders of magnitude, a high spatial resolution on the order of microns over a large area and a non-destructive readout are successfully demonstrated for the first time by combining the Ag-doped glass with LiF thin films.

2. Experimental details

2.1 Sample preparation and characterisation

A commercially available silver-doped phosphate glass dosimeter, GD-450 (Asahi Techno Glass Corporation), was used as a 2-D RPL detector. Although the weight composition of the 2-D detector was the same as that of the GD-450, i.e., 31.55 % P, 51.16 % O, 6.12 % Al, 11.00 % Na and 0.17 % Ag, the size and shape were different; the 2-D detector was a disk-type plate with a diameter of 80 mm and a thickness of 1 mm [12].

As a PL detector, LiF thin films deposited by a thermal evaporation technique on a borosilicate glass (BK-7) substrate were used. In addition, a commercially available X-ray imaging plate, BaFBr:Eu^{2+} (Fuji Photo Film), referred to as BAS-SR, was used for comparison as an OSL (or PSL) detector, which was attached to a disk-type BK-7 glass plate. The three kinds of disk-type detectors had the same diameter and thickness, with a 15-mm-diameter hole at the centre for rotation.

LiF thin films with a thickness of 1 μm were prepared as follows: LiF sintering pellets were used as the starting material. The substrate temperature was held constant during deposition at 200 and 300ºC. The present work did not aim to determine optimal conditions for the deposition rate, thickness or substrate temperature with respect to the structure and

morphology; therefore, the evaporation parameters were selected based on a previous investigation [13] of LiF thin films deposited on a glass substrate. The evaporation rate and vapour pressure in the chamber were 0.5 nm/s and 4.0×10^{-4} Pa, respectively.

To analyse the polycrystalline structure of the deposited LiF thin films, X-ray diffraction (XRD) patterns were recorded. In addition, the properties of the top surface (~10 nm thick), such as the chemical composition and the element bonding of the LiF films, were investigated by means of X-ray photoelectron spectroscopy (XPS).

In this work, the samples were coloured by irradiation from an X-ray unit (8.05 keV) with a copper target operating at 30 kV and 20 mA. The absorbed doses on the samples ranged from 1 to 126 Gy. Excitation (EXC), PL and RPL spectra were obtained at room temperature using a Hitachi F-4500 fluorescence spectrophotometer.

2.2 Imaging readout system

A schematic view of the experimental setup employed to measure the 2-D dose distributions is shown in Fig. 1. To read out the dose information on the detectors, an improved laboratory readout system with an optical pickup structure was employed. Collimated light at 371, 443 and 639 nm from continuous wave (CW) laser diodes (Coherent, Inc., Cube family) with a power of 3 mW was used as an excitation source for the RPL, PL and PSL detectors, respectively. The laser beam was expanded and reflected with a dichroic

beam splitter (B/S) and was focused on the vicinity of the surface of the disk-type detector by a Nikon LU Plan Fluor objective lens (×100, 0.90 NA) while reading out the image. The objective lens was simultaneously used both for laser excitation and emission collection. Each detector was attached to a spindle on a linear translation stage, which was rotated at a rate of 2400 rpm (40 Hz) and controlled to translate the laser beam spot from the outer to the inner disk in the radial direction with a pitch of 20 μm. Additional optical filters, including short-pass (SP) and long-pass (LP) filters, were inserted to reject the reflected emission and residual stimulating laser light, respectively. Only the signal was detected by the PMT, which then digitised the signal using a 500-kHz, 12 bit A/D converter. The dose distributions were reconstructed by a personal computer (PC). The total readout time was 1-7 minutes, depending on the track pitch (10-100 μm) and the number of tracks.

3. Results and discussion

We previously reported that each X-ray-induced band of silver-doped glasses can be attributed to silver-, phosphorous- and oxygen-related species on the basis of strong analogies with X-ray-irradiated silver-doped sodium chloride (NaCl:Ag) [14]. In addition, the origin, formation kinetics and optical properties of X-ray-induced Ag centres were also investigated through various methods [15, 16].

The EXC spectra (dashed and dotted lines) and the corresponding RPL spectra (solid and dash-dot lines) of an X-ray irradiated Ag-doped glass with a thickness of 0.3 mm under an absorbed dose of 1.0 Gy are shown in Fig. 2(a). The EXC spectra consisted of two different spectra, one with a peak at 310 nm for emission at 560 nm (the orange RPL) due to the Ag^{2+} centres and another with peaks at 270 and 340 nm, corresponding to a main emission at 470 nm (the blue RPL), due to the Ag_2^+ and Ag^0 centres, respectively. In this work, the blue RPL and some portion of the orange RPL were simultaneously emitted by an excitation wavelength of 371 nm from the laser diode.

Fig. 2(b) shows the EXC and PL spectra of an X-ray-irradiated LiF thin film with a thickness of 1 μm under an absorbed dose of 126 Gy. The attenuation length in LiF at the utilised energy of 8 keV is approximately 330 μm [17]; as a consequence, the films are entirely exposed to X-ray radiation. Although additional background noise from the coloured substrate was very weak, it was removed from the PL signal. The EXC spectra consist of two different peaks, one at 448 nm due to the F_3^+ centres and one at 444 nm due to the F_2 centres. Because these absorption bands almost overlap, these centres can be simultaneously excited with a single wavelength [7-9]. As a result, the PL spectra consist of two different Stokes-shifted emission bands peaking at 540 nm (the green PL) and 630 nm (the red PL), which correspond to the well-known positions of the F_3^+ and F_2 centres, respectively. Note that the ratios of the orange to blue RPL intensity (i.e., I_{orange}/I_{blue}) in Ag-doped glass and the red to

green PL intensity (i.e., I_{red}/I_{green}) in LiF are strongly sensitive to the radiation type, such as alpha-particles, beta- and X-rays and femtosecond (fs) lasers, as well as to the pulse duration, irradiation conditions at different temperatures and excitation photon energy [9, 18].

The optical characterisations of the Ag-doped glass, LiF films and BaFBr:Eu^{2+} materials used in this work based on the RPL, PL and PSL phenomena, respectively, are summarised in Table 1.

The LiF thin films were analysed by X-ray diffraction (XRD), with the results shown in Fig. 3. The XRD patterns were acquired for bulk LiF and LiF thin films deposited at substrate temperatures of 200 and 300ºC using a conventional Bragg-Brentano geometry and a grazing incidence (0.3°) geometry, respectively. The XRD patterns can be well indexed to the face-centred-cubic-structured LiF. Three diffraction peaks attributed to the (111), (200) and (220) LiF planes, corresponding to Bragg angles of 38.7, 45.0 and 65.5° for 2θ varying between 20 and 70°, were clearly observed. When the substrate temperature increases from 200 to 300ºC, the (200) peak intensity in the LiF thin films is higher. This result is in good agreement with previous observations [13] of LiF thin films evaporated on a glass substrate. In addition, this result confirms the suggestion [19] that the (200) plane has the lowest surface energy and is the most dense; therefore, the films grow along this crystalline direction once the energy is sufficiently high to allow for atom displacement at the surface.

Next, XPS measurements were performed for the Li 1s, F 1s, C 1s and O 1s core-level spectra for LiF thin films, with a LiF single crystal being used as a reference. Only the XPS spectra of the Li 1 s and F 1s core levels are shown in Fig. 4. Accounting for the photoelectron energy drift due to the charging effect, the binding energy (BE) scale was calibrated in reference to the C 1s peak (284.6 eV). All of the shapes of the Li 1s line were symmetric, and there was no shoulder from the lower BE side that could be assigned to the presence of the Li bulk plasmon, which would indicate a metallic character, as observed in [20].

Fig. 5 shows a set of the reconstructed dose distributions obtained from the X-ray-irradiated disk-type Ag-doped glasses (based on the RPL), LiF thin films (PL) deposited on a glass substrate and BaFBr: Eu^{2+} (PSL) attached to a glass plate detectors with absorbed doses of 3.5, 49.2 and 3.5 Gy, respectively, using the homemade imaging readout system. In the cases of the RPL and PL detectors, all of the optics used for signal detection, except for the stimulating laser (371 nm, 443 nm), were nearly the same. In the reconstructed images, the red regions of the colour axes correspond to higher concentration levels, while the blue regions indicate areas in which soft X-rays passed through 250-μm-thick stainless steel or several Al foil layers (17 μm thick) attached to the detectors as a mask or as non-exposure parts during X-ray irradiation. In the case of the RPL detector, steep gradients of dose distribution levels are

clearly resolved with the highest image contrast. In the case of the PL detector, X-ray radiation doses up to approximately 10 Gy were required to reconstruct the dose distributions.

As previously reported [21, 22], the F_2 and F_3^+ centre productions in gamma ray irradiated LiF thin films and bulk LiF with doses from 10^3 to 10^5 Gy are linear on a log-log scale, and a saturation effect is observed above 10^5 Gy. As a result, it may be possible to realise a wide dynamic range of 11 orders of magnitude through the use of Ag-doped glass (dose range of 10^{-6}-10^1 Gy) and LiF thin films (dose range of 10^1-10^5 Gy). In contrast, in the case of the PSL detector, it was very difficult to adjust the optimised position between the surface of the detector and the objective lens while reading out the image, as the detector exhibits high fading and its stored information is lost after the first-readout run.

In addition, based on the radiation-induced Ag-related colour centres (Ag^0 and Ag^{2+} CCs in Ag-doped glass) and F-aggregated colour centres (F_2 and F_3^+ CCs in LiF), the intrinsic spatial resolution of the Ag-doped glass and LiF detectors will be several nanometers [7-9]. However, in the present study, the resolution is limited by the readout system utilised for the RPL and PL detectors. Nevertheless, the dose distribution images obtained for the Ag-doped glass detector were reconstructed with a spatial resolution of ~1 μm and a sensitivity of 1 mGy using the prototype reading system [12]. In contrast, in the case of the BaFBr:Eu^{2+} detector, which consists of a plastic plate coated with fine PSL crystals (~5 μm), BaFBr:Eu^{2+},

combined in an organic binder, the spatial resolution (typically, ~25 μm) of the BaFBr:Eu^{2+} detector is expected to be inferior to that of the other two detectors.

The advantages and disadvantages of the PSL, PL and PSL detectors were evaluated and verified from the X-ray dose distributions and are summarised in Table 2.

The values of the effective atomic number, Z_{eff}, of the Ag-doped glass, LiF thin films and BaFBr:Eu^{2+} materials are also presented in Table 2. The Z_{eff} value is often used to describe the extent to which a material approximates or deviates from soft tissue in its interaction with a photon radiation field [2, 4], which is an important parameter in medical applications. It is well known that the Z_{eff} value of TL materials such as LiF:Mg, Ti and $Li_2B_4O_7$ is close to that of soft tissue (Z_{eff} =7.35), which is termed tissue equivalent. The Z_{eff} value of the Ag-doped glass is calculated to be 12.57. Therefore, the Ag-doped glass detector shows an over-response of the dose for low-energy photons (< 100 keV) due to photoelectric absorption. To correct the over-response in the low-energy range, Manninen *et al*. [23] reported that a filter composed of tin (Sn) is useful for energy compensation in the diagnostic energy range (50-125 keV), while the filter is not required in the radiation therapy energy range (6-15 MeV) when using commercially available GD-352M and GD-302M (Asahi Techno Glass Corporation) type glasses based on the RPL phenomena.

4. Conclusions

The data obtained in this study led to the following conclusions:

(1) A novel disk-type Ag-doped phosphate glass and LiF thin film detectors were proposed and demonstrated for the first time. Each detector is based on the high luminescence efficiency of the RPL and PL phenomena.

(2) The capabilities of the 2-D dose images accumulated with a high spatial resolution over a large area, a wide dynamic range covering 11 orders of magnitude and a non-destructive readout are successfully demonstrated by combining the Ag-doped glass with LiF thin films. Such a dosimeter capable of measuring doses from very low to high levels should be particularly suitable for X-ray and gamma ray imaging in radiation diagnostics and clinical radiotherapy, respectively.

(3) The area sizes and shapes are not limited by the functionality or controllability of the host materials on the glass, such as Ag-doped glass or LiF thin films. At present, disk-type detectors with larger dimensions (12 cm diameter) are being employed for medical applications. In addition, further tests of the energy compensation of Ag-doped glass in the low-energy range and three-dimensional (3-D) reconstructed images are underway.

References

[1] T. Yamamoto, D. Maki, F. Sato, Y. Miyamoto, H. Nanto, T. Iida, Radiat. Meas. 46 (2) (2011) 1554-1559.

[2] E. G. Yukihara, S. W. S. McKeever, Optically Stimulated Luminescence, John Wiley & Sons (2011).

[3] P. Olko, Radiat. Meas. 45 (3-6) (2010) 506-511.

[4] A. J. J. Bos, Nucl. Instr. Meth. Phys. Res. B 184 (1-2) (2001) 3-28.

[5] J. H. Lee, M. S. Lin, S. M. Hsu, I. J. Chen, W. L. Chen, C. F. Wang, Radiat. Meas. 44 (1) (2009) 86-91.

[6] Y. Garcier, G. Cordier, C. Pauron, J. Fazileabasse, Radiat. Prot. Dosim. 124 (2) (2007) 107-114.

[7] G. Baldacchini, F. Bonfigli, A. Faenov, F. Flora, R. M. Montereali, A. Pace, T. Pikuz, L. Reale, J. Nanosci. Nanotech., 3(6) (2003) 483-486.

[8] R. M. Montereali, S. Almaviva, F. Bonfigli, A. Cricenti, A. Faenov, F. Flora, P. Caudio, A. Lai, S. Martellucci, E. Nichelatti, T. Pikuz, L. Reale, M. Richetta, M. A. Vincenti, Nucl. Instr. Meth. Phys. Res. A 623 (2) (2010) 758-762.

[9] T. Pikuz, A. Faenov, Y. Fukuda, M. Kando, P. Bolton, A. Mitrofanov, T. A. Vinogradov, M. Nagasono, H. Ohashi, M. Yabashi, K. Tono, Y. Senba, T. Togashi, T. Ishikawa, Opt. Express 20 (4) (2012) 3424-3433.

[10] G. M. Akselrod, M. S. Akselrod, E. R. Benton, N. Yasuda, Nucl. Instr. Meth. Phys. Res. B 247 (2) (2006) 295-306.

[11] D. Maki, T. Nagai, F. Sato, Y. Kato, T. Yamamoto, T. Iida, Radiat. Meas. 46 (2) (2011) 1543-1546.

[12] T. Kurobori, S. Nakamura, Radiat. Meas. 47 (10) (2012) 1009-1013.

[13] R. M. Montereali, G. Baldacchini, S. Martell, L. C. Scavarda do Carmo, Thin Solid Films 196 (1) (1991) 75-83.

[14] T. Kurobori, W. Zheng, Y. Miyamoto, H. Nanto, T. Yamamoto, Opt. Mater. 32 (9) (2010) 1231-1236.

[15] W. Zheng, T. Kurobori, J. Lumin. 131 (1) (2011) 36-40.

[16] W. Zheng, T. Kurobori, Nucl. Instr. Meth. Phys. Res. B 269 (23) (2011) 2814-2818.

[17] The centre for X-ray Optics, “X-ray interactions with matter”, http://henke.lbl.gov/optical_constants.

[18] T. Kurobori, T. Yamakage, Y. Hirose, K. Kawamura, M. Hirano, H. Hosono, Jpn. J. Appl. Phys. 44 (2) (2005) 910-913.

[19] F. Cosset, A. Celerier, B. Barelaud, J-C. Vareille, Thin Solid Films 303 (1-2) (1997) 191-195.

[20] R. M. Montereali, F. Bonfigli, V. Mussi, E. Nichelatti, A. Santoni, S. Scaglione, IOP Conf. Series: Mater. Sci. Eng. 15(1) (2010) 012017-012022.

[21] A. Perez, E. Balanzat, J. Dural, Phys. Rev. B 41 (7) (1990) 3943-3950.

[22] R. M. Montereali, T. Marolo, M. Montecchi, E. Nichelatti, Nucl. Instr. Meth. Phys. Res. B 268 (19) (2010) 2866-2869.

[23] A. L. Manninen, A. Koivula, M. T. Nieminen, Radiat. Prot. Dosim. 151 (1) (2012) 1-9.

TABLE CAPTIONS:

Table 1

Summary of RPL, PL and OSL (PSL) materials and relevant optical properties used in this work.

Table 2

Advantages and disadvantages of Ag-doped glass (RPL), LiF thin films (PL) and BaFBr: Eu^{2+} (PSL) detectors obtained in this work.

FIGURE CAPTIONS:

Fig. 1
(Color online) Schematic diagram of a disk-type RPL, PL and PSL readout system (not to scale).

Fig. 2
EXC and RPL spectra of Ag-doped glass (a) after X-ray irradiation with an absorbed dose of 1 Gy. EXC and PL spectra of X-ray-irradiated LiF thin films (b) after X-ray irradiation with an absorbed dose of 126 Gy.

Fig. 3
Bragg-Brentano X-ray diffraction spectrum of bulk LiF (a). Grazing incidence X-ray diffraction spectra of 1-μm-thick LiF films deposited at 300ºC (above) and 200ºC (bottom) onto a glass substrate (b).

Fig. 4
XPS spectra of Li 1s (a) and F 1s (b) core levels for bulk LiF and LiF films deposited at substrate temperatures of 300ºC (above) and 200ºC (bottom).

Fig. 5
(Color online) Reconstructed 2-D dose distributions acquired using the X-ray irradiated disk-type Ag-doped glass (a), LiF thin films (b) and BaFBr: Eu^{2+} (c) detectors with absorbed doses of 3.5, 49.2 and 3.5 Gy, respectively.

1-column

Table 1 T. Kurobori

Material	Phenomena	Excitation wavelength, nm (centres)	Emission wavelength, nm (lifetime: ns)
Ag-doped glass	RPL	310 (Ag^{2+})	560 (2000)
		340 (Ag^{0})	460 (5)
LiF thin film	PL	444 (F_2)	630 (16)
		448 (F_3^+)	540 (8)
$BaFBr:Eu^{2+}$ (BAS-SR)	OSL	590 $F(Br^-)$	390 (800)
		490 $F(F^-)$	

	Ag-doped glass	LiF thin film	$BaFBr:Eu^{2+}$
Spatial resolution	◎ <1 μm	◎ <1 μm	△ ~25 μm
Sensitivity	◎	△	◎
Fading effect	◎	◎	×
Dynamic range	◎ 10^{-4} - 10^{1} Gy	○ 10^{1} - 10^{4} Gy	◎ 10^{-4} - 1 Gy
Reuse	○ 400°C, 30 min	○ 400°C, 30 min	◎ white light
Effective atomic number	△ ~12.57	○ ~8.25	× ~50

Figure

2-column or 1.5-column (Color online)

Figure 1 T. Kurobori

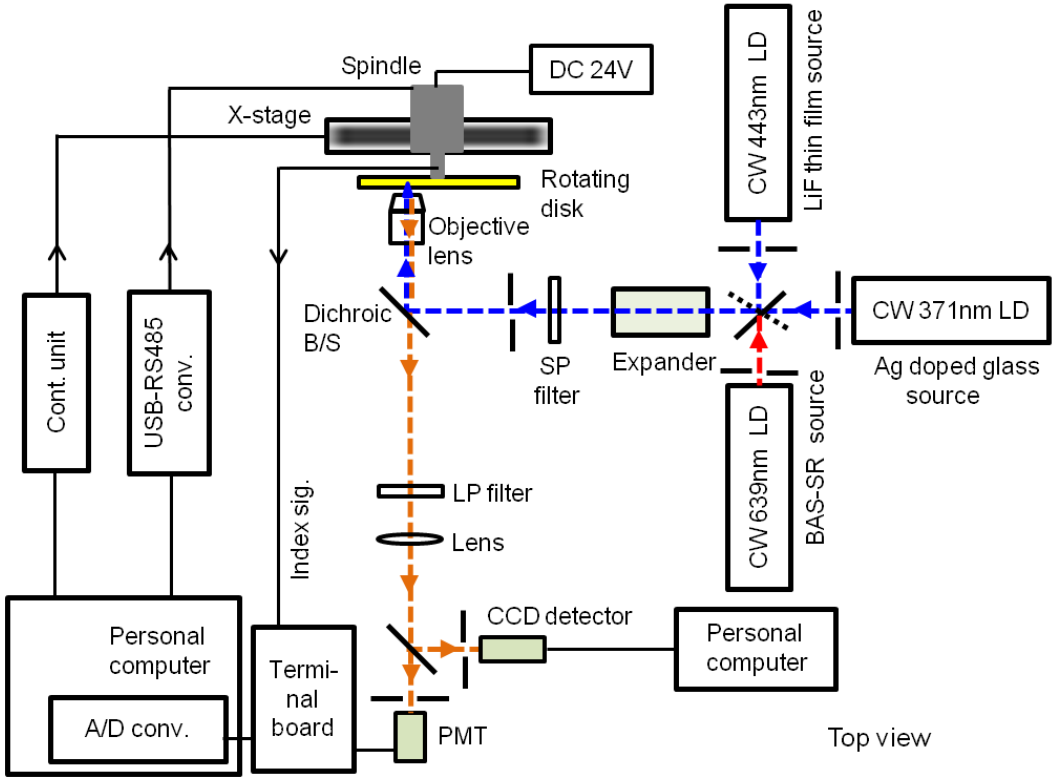

1-column

Figure 2 T. Kurobori

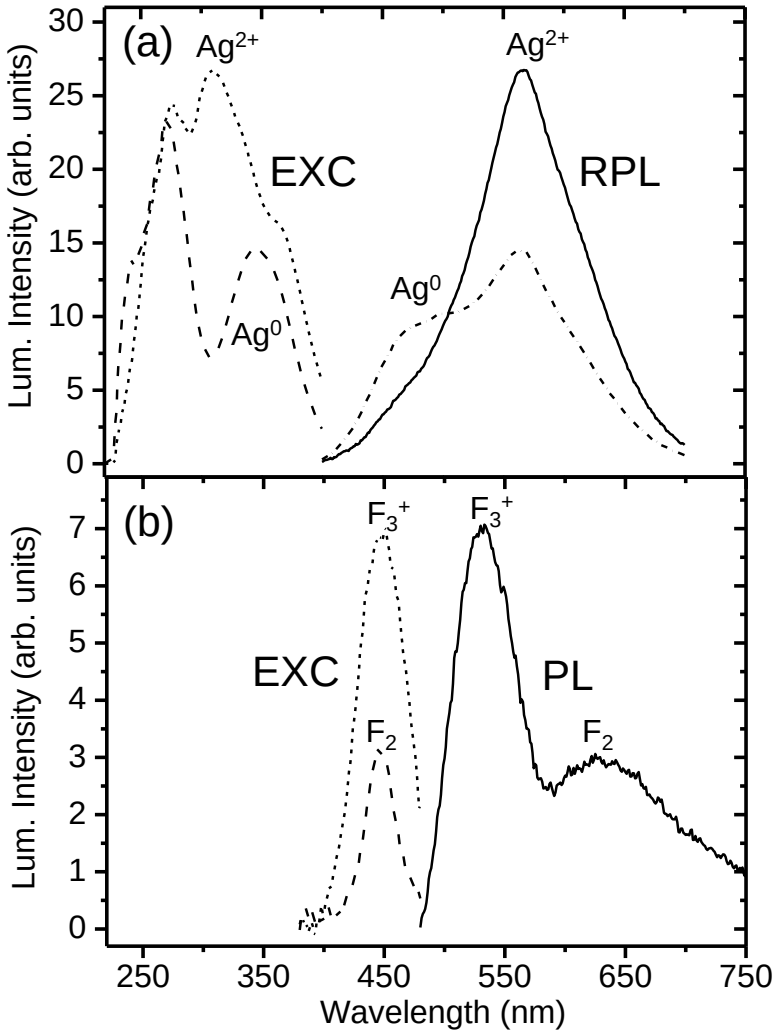

1-column

Figure 3 T. Kurobori

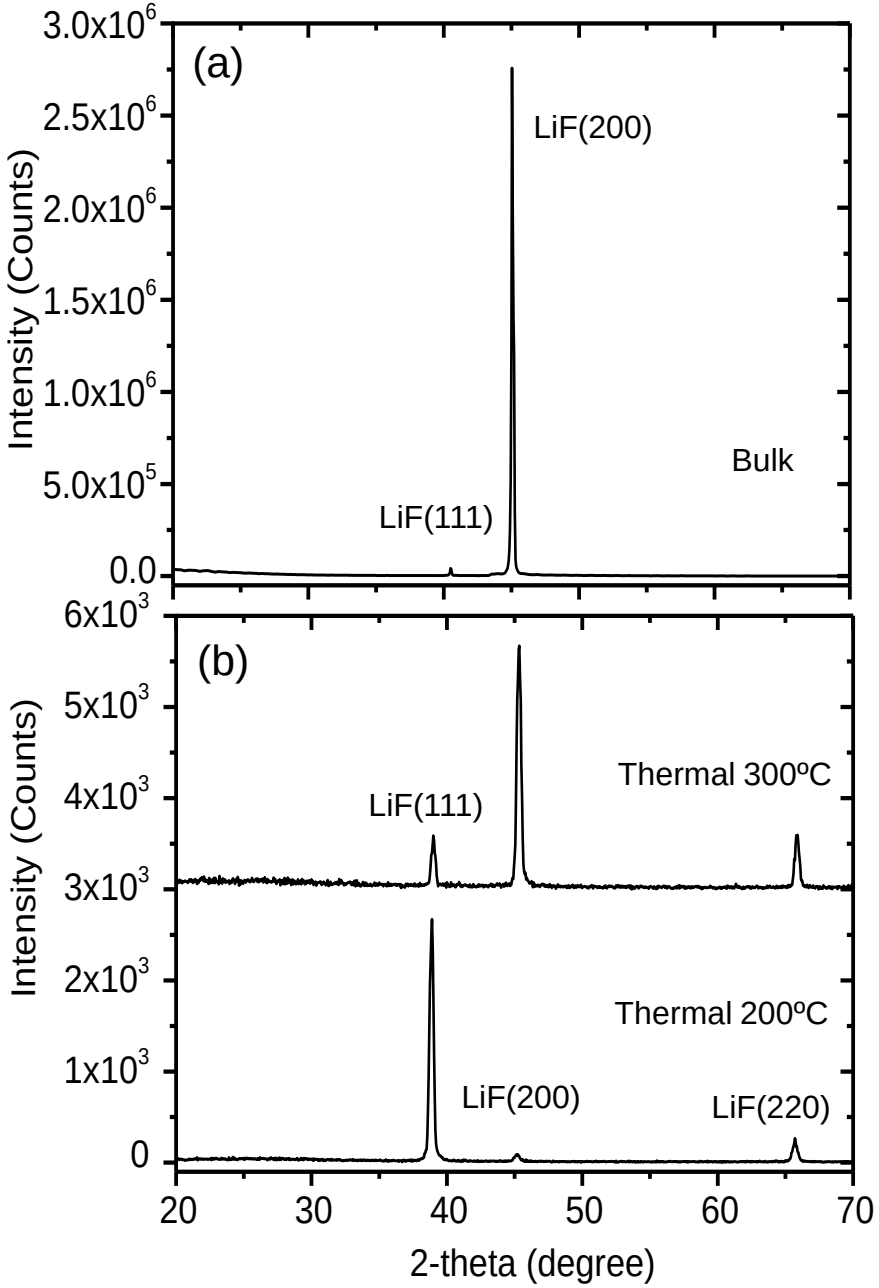

1-column

Figure 4 T. Kurobori

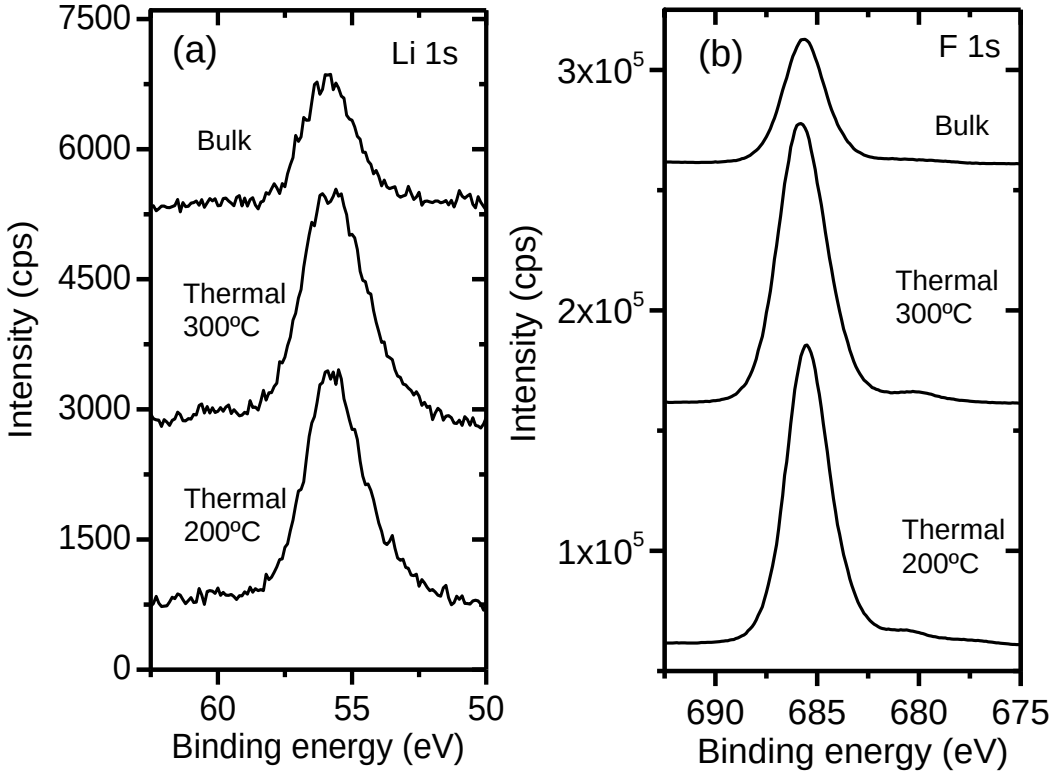

2-column or 1.5-column (Color online)

Figure 4 T. Kurobori